Journal of Luminescence 131 (2011) 78–82

Contents lists available at ScienceDirect

Journal of Luminescence

journal homepage: www.elsevier.com/locate/jlumin

Efficient and color-saturated inverted bottom-emitting organic light-emitting devices with a semi-transparent metal-assisted electron injection layer

Meng-Huan Ho [a,*], Chang-Yen Wu [b], Teng-Ming Chen [a], Chin H. Chen [c]

[a] Department of Applied Chemistry, National Chiao Tung University, 210 R, CPT Building, 1001 Ta Hsueh Road, Hsinchu 300, Taiwan, ROC
[b] Department of Photonics, National Chiao Tung University, Hsinchu 300, Taiwan, ROC
[c] Display Institute, Microelectronics and Information Systems Research Center, National Chiao Tung University, Hsinchu 300, Taiwan, ROC

ARTICLE INFO

Article history:
Received 18 January 2010
Received in revised form
30 August 2010
Accepted 3 September 2010
Available online 15 September 2010

Keywords:
Organic light-emitting diodes
Inverted
Bottom-emitting
Microcavity

ABSTRACT

We report the development of highly efficient and color-saturated green fluorescent 10-(2-benzothiazolyl)-1,1,7,7-tetramethyl-2,3,6,7-tetrahydro-1*H*,5*H*,11*H*-benzo[*l*]pyrano-[6,7,8-*ij*]quinolizin-11-one dye-doped inverted bottom-emitting organic light-emitting diode (IBOLED). This was enabled by the insertion of a silver (Ag) based semi-transparent metal-assisted electron injection layer between the ITO cathode and *n*-doped electron transporting layer. This IBOLED with ITO/Ag bilayer cathode with its synergistic microcavity effect achieved luminous efficiencies of 20.7 cd/A and 12.4 lm/W and a saturated $CIE_{x,y}$ of (0.22, 0.72) at 20 mA/cm^2, which are twice better than those of the conventional OLED and have over 60% improvement on IBOLED without ITO/Ag bilayer cathode.

1. Introduction

Due to their superb image quality, large viewing angle, high power efficiency and capability of displaying near flawless full motion video, active-matrix organic light-emitting diodes (AMOLEDs) have emerged as one of the main contenders of the next-generation information flat panel displays [1,2]. At the same time, amorphous silicon thin-film transistors (*a*-Si TFTs) have shown considerable promise as backplane for large AMOLEDs displays such as OLED-TV. In addition, the next generation amorphous-oxide TFT appears to have neither instability issues of mobility nor sub-threshold gate voltage swing (down to 0.20 V/dec) and exhibit large carrier mobility ($\sim$10 cm^2/V s) [3–6]. Moreover, oxide TFTs can be deposited at much lower temperature, which in principle makes possible the mass production of AMOLEDs on flexible plastic substrates.

However, it appears that both amorphous silicon and amorphous oxide are *n*-type semiconductors, which are best used to fabricate *n*-channel TFTs. As a result, the bottom anode of conventional OLEDs can only be fabricated at the source end of the driving *n*-channel TFTs, which would invariably impact the stability of the source voltage that intimately connected to the voltage drop across the OLED materials. The most direct way of solving this problem is to use an inverted type OLED (IOLED) for *n*-channel TFTs as it enables the direct connection between the bottom cathode and the *n*-channel TFT drain line, which may ultimately result in a decrease in driving voltage and thus improved stability [7–9]. Accordingly, research and development of IOLEDs have become increasingly important and timely toward the realization of *a*-Si TFT or oxide TFT driven large panel AMOLEDs.

Typical OLEDs possess a transparent electrode indium-tin-oxide (ITO) with high work function for anode and an opaque reflective metal for cathode such as LiF/Al [10]. For inverted type bottom-emitting OLED (IBOLEDs) devices, however, ITO has to be inverted to function as cathode, which creates some problems as the electron is difficult to be injected from ITO into the organic layer due to their severe energy levels mismatch, which in turn would cause the drive voltage to rise sharply and efficiency to fall. The problem can be overcome by evaporating an ultrathin layer of magnesium (Mg) or introducing the lithium (Li) and cesium (Cs) doped 4,7-diphenyl-1.10-phenanthroline (BPhen) layer onto ITO to reduce the electron injection barrier from the ITO cathode and further enhance device performance [7,11].

However there yet exist some other problems, for example, the ultrathin Mg and active Li and Cs are rather difficult to handle and deposit. Moreover, conversion of photons generated within the device into external visible light is still a challenge. It is well known that outcoupling efficiency and color saturation of OLEDs can be enhanced by microcavity in top-emitting OLED between a high-reflection back electrode and a semi-transparent metallic

* Corresponding author. Tel.: +886 3 5712121x52919; fax: +886 3 573 5601.
E-mail address: kinneas.ac94g@nctu.edu.tw (M.-H. Ho).

0022-2313/$ - see front matter © 2010 Elsevier B.V. All rights reserved.
doi:10.1016/j.jlumin.2010.09.002

ground contact [12,13]. Here, we demonstrate enhanced light outcoupling by intentionally creating a microcavity within the IBOLEDs, which is accomplished by inserting an easily deposited and thin semi-transparent silver (Ag) layer between ITO and the *n*-doped ETL of 4,7-diphenyl-1,10-phenanthroline (BPhen): 10% cesium carbonate (Cs_2CO_3). Using this concept in our OLED design, we also found that the inserted thin Ag layer not only enhances color saturation as expected but also increases electron injection.

2. Experimental

Fig. 1 depicts the structure of OLED devices in this study. In our experiments, two 10-(2-benzothiazolyl)-1,1,7,7-tetramethyl-2,3,6,7-tetrahydro-1*H*,5*H*,11*H*-benzo[*l*]pyrano-[6,7,8-*ij*]quinolizin-11-one (C-545T) green-doped IBOLED devices I and II are fabricated, whose structures were ITO (cathode)/4,7-diphenyl-1,10-phenanthroline (BPhen): 20% cesium carbonate (Cs_2CO_3) (12 nm)/*tris*(8-hydroxyquinoline)aluminum (Alq_3) (18 nm)/Alq_3: 1% C545T (30 nm)/*N,N′*-bis-(1-naphthyl)-*N,N′*-diphenyl,1,1′-biphenyl-4,4′-diamine (NPB) (30 nm)/NPB: 33% tungsten oxide (WO_3) (5 nm)/WO_3 (5 nm)/Al (anode, 100 nm) and ITO (cathode)/Ag (20 nm)/BPhen: 20% Cs_2CO_3 (5 nm)/Alq_3 (18 nm)/Alq_3: 1% C545T (30 nm)/NPB (30 nm)/NPB: 33% WO_3 (5 nm)/WO_3 (5 nm)/Al (anode, 100 nm), respectively. In the device architecture, BPhen: 20% Cs_2CO_3 (5 nm) and NPB: 33% WO_3 (5 nm)/WO_3 (5 nm) were used as the *n*-doped electron transport layer (*n*-ETL) and *p*-doped hole transport layer (*p*-HTL), respectively. For comparison, a conventional OLED device was also fabricated with the structure of ITO (anode)/CF_x/NPB (70 nm)/Alq_3: 1% C545T (37.5 nm)/Alq_3 (37.5 nm)/LiF (1 nm)/Al (100 nm).

For studying the electron injection phenomenon, the following electron-only devices were fabricated with structures of ITO/Alq_3 (80 nm)/Al (100 nm) (standard device, no electron injection layer) and ITO/Ag (0, 1, 10, 20, 30 nm)/BPhen: 10% Cs_2CO_3 (20 nm)/Alq_3 (80 nm)/Al (100 nm), respectively.

Reflection and transmission spectra were measured by the PerkinElmer Lambda 950. The work function was estimated from the threshold energy of ultraviolet photoelectron spectrum by using model AC-2 (RKI Instruments, Inc.) to test the sample surface in the air.

After a routine cleaning procedure, the indium-tin-oxide (ITO)-coated glass was loaded on the grounded electrode of a parallel-plate plasma reactor, pretreated by oxygen plasma, and then coated with a polymerized fluorocarbon film. Devices were fabricated under the base vacuum of about 10^{-6} Torr in a thin-film evaporation coater following a published protocol [14]. In the evaporation of EML, the fluorescent dopant was co-deposited with the host molecule at its optimal molar ratio. After the thermal deposition of the organic layers and without a vacuum break, the ultrathin layer of 1 nm of LiF was followed by 200 nm of Al deposition through a patterned shadow mask on top of the organic layers using separately controlled sources to complete the cathode. All devices were hermetically sealed with a glass cap and UV glue prior to testing. The active area of the EL device, defined by the overlap of the ITO and the cathode electrodes, was 9 mm^2. The current–voltage–luminance characteristics of the devices were measured with a diode array rapid scan system using a Photo Research PR650 spectrophotometer and a computer-controlled programmable dc source. The device lifetime measurements were performed in ambient environment at a constant drive current density.

3. Results and discussion

3.1. Using Ag thin film as electron injection layer

Cesium carbonate (Cs_2CO_3), either vacuum deposited as the electron injection layer (EIL) or doped and dispersed in electron transporting molecules such as BPhen and Alq_3, has shown improved electron injection and transport properties, and thereby has often been applied in conventional OLEDs [3,15]. In this study, we deposited a layer of BPhen: 10% Cs_2CO_3 on ITO cathode to improve the electron injection efficiency to overcome the high electron injection barrier due to the high work function of the ITO cathode. To study the electron injection phenomenon, the current density–voltage (*J–V*) characteristics of electron-only devices were investigated as shown in Fig. 2. It is evident that standard device without the electron injection layer shows much lower electron current due to the high electron injection barrier between ITO and Alq_3, while the electron current is greatly enhanced by introducing a BPhen: Cs_2CO_3 interfacial layer between ITO and Alq_3.

To further enhance the electron injection from the ITO cathode, we deposited a thin Ag layer, which has a low work function of 4.5–4.7 eV [16], upon ITO as a bilayer cathode and fabricated a series of electron-only devices with various Ag thicknesses. The *J–V* characteristics of these electron-only devices are also shown in Fig. 2. It is obvious that the drive current can be further improved at the same voltage when the thickness of Ag layer is greater than 10 nm. We also measured the work function of ITO/Ag samples by ultraviolet photoelectron spectroscopy (Model AC-2) as shown in Fig. 3. The result shows that the surface work function of ITO/Ag samples is all in the range of 4.85–4.89 eV, which is lower than that of the neat ITO (5.16 eV) and indicates that the inserted Ag thin layer can greatly reduce the electron injection barrier from the ITO cathode, thus further enhancing the electron injection current.

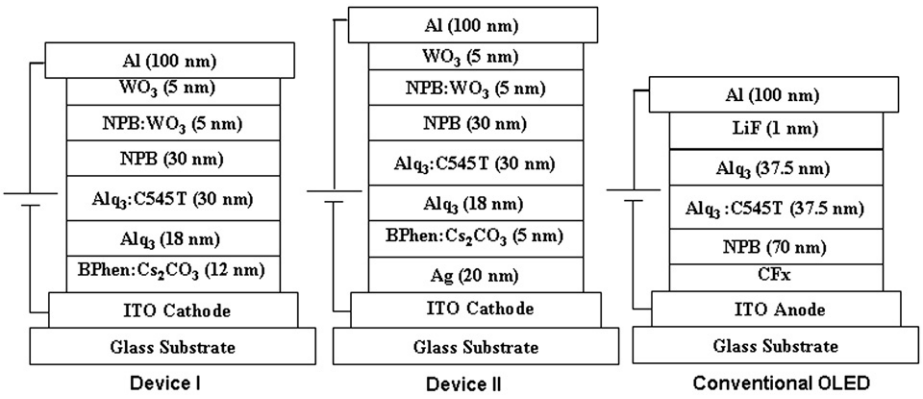

Fig. 1. Structures of IBOLED devices I, II and conventional OLED device.

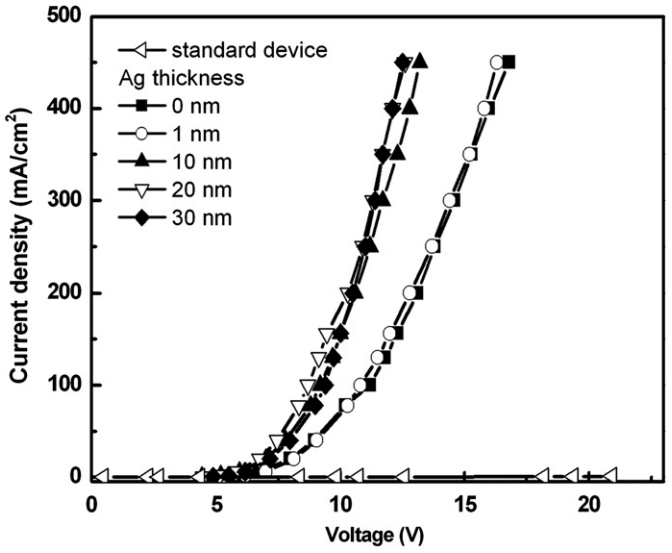

Fig. 2. Current density–voltage (J–V) characteristics of electron-only devices.

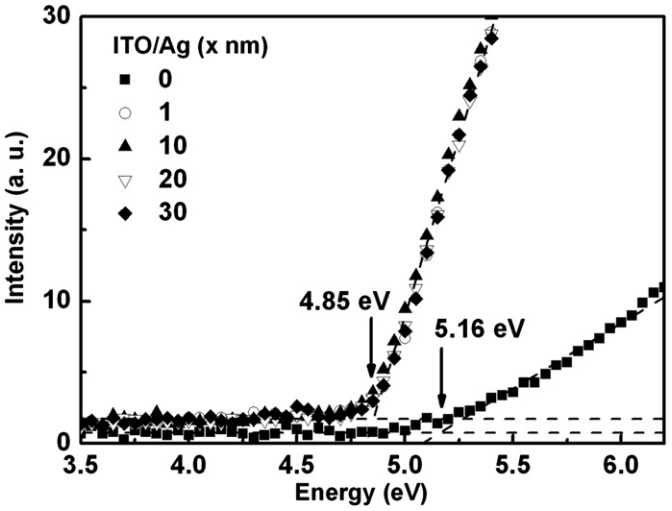

Fig. 3. Photoelectron spectra of ITO/Ag samples.

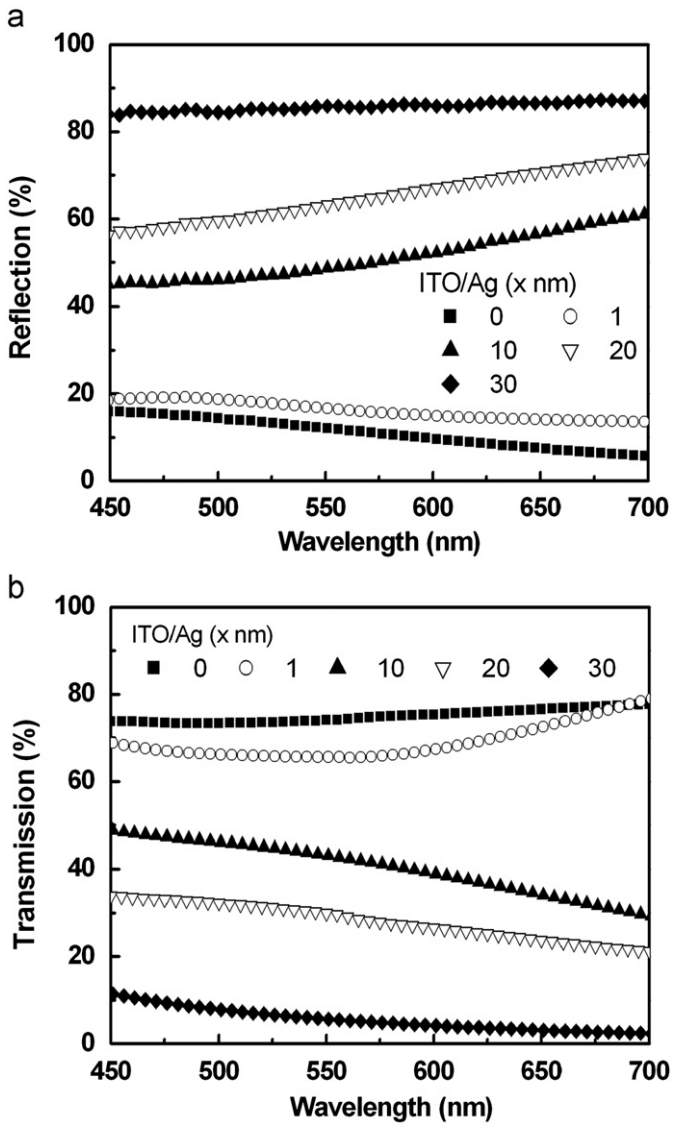

Fig. 4. Optical properties of different thicknesses of silver layer on ITO cathode: (a) reflection and (b) transmission.

3.2. Optical properties of ITO/Ag bilayer cathode

Fig. 4(a) and (b) shows the optical reflection and transmission spectra of ITO/Ag samples with different Ag thicknesses. The reflectance of ITO/Ag bilayer cathode was found to increase while the transmission decreased with Ag thickness. When the Ag thickness was increased to 30 nm, the transmission of ITO/Ag bilayer cathode was even lower than 20% across the visible spectrum from 450 to 700 nm. It is well known that incorporating well designed microcavity structures in OLEDs can provide up to twofold enhancement in luminance efficiency through redistributing radiation generated in devices [11,12]. For a typical microcavity device, a high-reflection back mirror and a low-loss high-reflection exit mirror are essential to enhance emission around a certain wavelength and obtain luminance enhancement. In our IBOLED devices, Al was used as a top anode as well as the high-reflection back mirror with a reflectance of 0.9. Furthermore, it can be seen that the absorption of ITO/Ag samples is all quite low with values of 0.1–0.15 from 450 to 700 nm ($A=1-T-R$). Therefore, according to the previous results of Lin et al. [17], the inserted Ag thin layer of 20 nm is expected not only to be used for electron injection layer but also to function as a low-loss high-reflection exit mirror in our device architecture.

3.3. Performance of inverted bottom-emitting devices

Detailed electroluminescent (EL) performances of these devices measured at 20 mA/cm^2 are summarized in Table 1. Both IBOLED devices I and II show the lower drive voltage and dramatic gain in power efficiency as compared with those of the conventional device. We attribute the lower drive voltage to the use of BPhen doped Cs_2CO_3 layer between ITO and Alq_3 as well as the NPB doped WO_3/WO_3 bilayer composition in the inverted OLED device structure that can effectively improve the carrier injection from both electrodes into the organic layers. Therefore, device I also shows a better power efficiency of 7.7 lm/W than that of the conventional device (5.2 lm/W). Fig. 5 shows the EL spectra of devices I, II and the conventional device at 20 mA/cm^2. It is found that device II emitted a more saturated green color at 524 nm with a narrower full width at half maximum (FWHM) of

Table 1
EL performances of devices I, II and conventional device driven at 20 mA/cm^2.

Device	Voltage (V)	Luminance (cd/m^2)	Current eff. (cd/A)	Power eff. (lm/W)	E.Q.E. (%)	CIE$_{x,y}$
I	**5.3**	**2602**	**13**	**7.7**	**3.5**	**(0.29, 0.65)**
II	**5.2**	**4149**	**20.7**	**12.4**	**5.4**	**(0.22, 072)**
Conventional	**6.1**	**2033**	**10.1**	**5.2**	**2.8**	**(0.33, 0.62)**

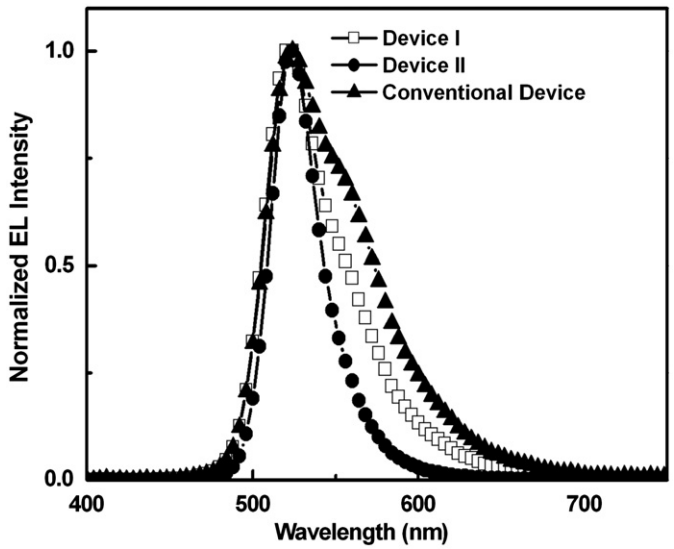

Fig. 5. Normalized EL spectra of devices I, II and conventional device at 20 mA/cm^2.

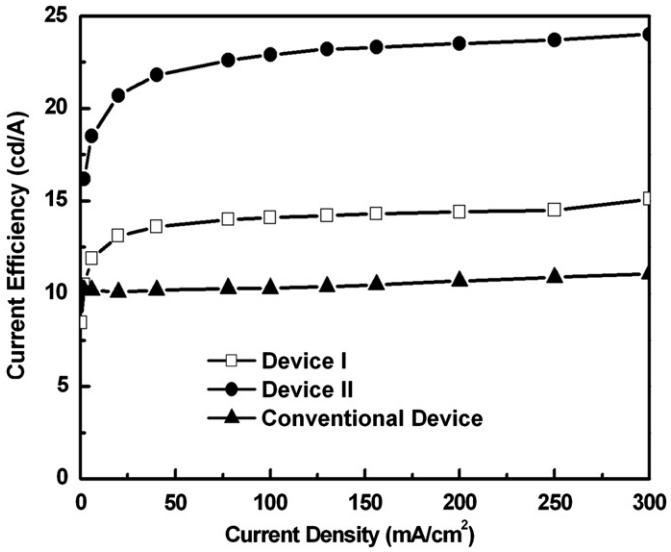

Fig. 6. Current efficiency versus current density characteristics of devices I, II and conventional device.

32 nm and CIE$_{x,y}$ color coordinates of (0.22, 0.72) than those of the conventional device. We attribute this phenomenon to the insertion of the semi-transparent ITO/Ag bilayer, which can be regarded as a low-loss high-reflection exit mirror to enhance emission around a certain wavelength in IBOLED device architecture. As a result, we effectively create a cavity device with ITO/Ag bilayer cathode and further enhance the luminance and color saturation in the forward direction.

Fig. 6 shows the current efficiency versus current density characteristics of these three devices, among which device II with ITO/Ag bilayer is seen to achieve the highest efficiency of 20.7 cd/A and 12.4 lm/W. This IBOLED with ITO/Ag bilayer cathode with its synergistic microcavity effect was able to achieve maximum efficiencies that are twice as high as those of the conventional OLED and there was over 60% improvement on IBOLED without Ag thin film. These results indicate that the Ag assisted electron injection layer improves not only the electrical properties but also the optical properties by simultaneously creating a microcavity effect in the IBOLEDs from which dramatic enhancement in color saturation can also be obtained.

We also measured the device operational lifetime of device II in the ambient environment. The $t_{1/2}$ [the time for the luminance to drop to 50% of initial luminance (L_0)] of device II measured at constant current densities of 20 mA/cm^2 (L_0=4150 cd/m^2) and 50 mA/cm^2 (L_0=11000 cd/m^2) were 1610 and 300 h, respectively. Assuming scalable Coulombic degradation of ($L_0^n \times T_{1/2}$=constant) under accelerated drive conditions [18], the acceleration factor (n) of device II has been estimated to be about 1.72, as depicted in Fig. 7. By estimation of the extrapolated profile, the $t_{1/2}$ of device II driving at an L_0 value of 1000 cd/m^2 is projected to be about 17,380 h. The remarkably long operational lifetime is attributed to the improved electron injection by the inserted Ag thin layer on the ITO surface, which leads to much reduced fluorescent quenching of the Alq_3 cationic radical [19–21] produced by the excess hole in the emitter.

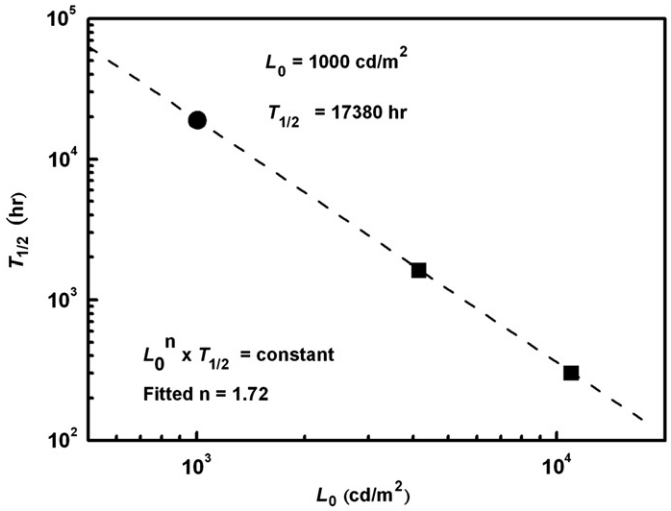

Fig. 7. Extrapolated half-life of device II.

4. Conclusion

Study of IOLEDs has become increasingly important and timely toward the realization of an *a*-Si TFT or oxide TFT driven large panel AMOLED such as OLED-TV. This is because it provides a bottom cathode that can be connected to the drain end of the *n*-channel TFT through which the current circuit of the TFT can be decoupled from the resistive loss of the OLED materials. We have demonstrated that both power efficiency and color saturation in IBOLED can be enhanced by inserting an easily deposited and semi-transparent metal-assisted electron injection layer between

ITO and the *n*-doped ETL, thus creating a beneficial microcavity effect, which can be exploited to enhance color saturation as well without impacting its electrical property. The efficiency of this IBOLED was boosted up to 20.7 cd/A and 12 lm/W and also saturate green $CIE_{x,y}$ coordinates of (0.22, 0.72) were achieved with a long operational lifetime of 17,380 h at $L_0=100$ cd/m^2.

Acknowledgement

The authors gratefully acknowledge the support of AU Optronics Corporation, Hsinchu, Taiwan, for funding of this work. EL grade OLED materials were provided by the e-Ray Optoelectronics, Co. Ltd., Chungli, Taiwan.

References

[1] H.K. Chung, K.Y. Lee, SID Symposium Digest of Technical Papers, vol. 36, 2005, p. 956.
[2] S.T. Lee, M.C. Suh, T.M. Kang, Y.G. Kwon, J.H. Lee, H.D. Kim, H.K. Chung, SID Symposium Digest of Technical Papers, vol. 38,(2007, p. 1588.
[3] J.K. Jeong, J.H. Jeong, J.H. Choi, J.S. Im, S.H. Kim, H.W. Yang, K.N. Kang, K.S. Kim, T.K. Ahn, H.-J. Chung, M. Kim, B.S. Gu, J.-S. Park, Y.-G. Mo, H.D. Kim, H.K. Chung, SID Symposium Digest of Technical Papers, vol. 39, 2008, p. 1.
[4] K. Nomura, H. Ohta, K. Ueda, T. Kamiya, M. Hirano, H. Hosono, Science 300 (2003) 1269.
[5] K. Nomura, H. Ohta, A. Takagi, T. Kamiya, M. Hirano, H. Hosono, Nature 432 (2004) 488.
[6] M. Kim, J.H. Jeong, H.J. Lee, T.K. Ahn, H.S. Shin, J.S. Park, J.K. Jeong, Y.G. Mo, H. Do Kim, Appl. Phys. Lett. 90 (2007) 212114.
[7] T.Y. Chu, J.F. Chen, S.Y. Chen, C.J. Chen, C.H. Chen, Appl. Phys. Lett. 89 (2006) 053503.
[8] V. Bulovi, P. Tian, P.E. Burrows, M.R. Gokhale, S.R. Forrest, Appl. Phys. Lett. 70 (1997) 2954.
[9] X. Zhou, M. Pfeiffer, J.S. Huang, J. Blochwitz-Nimoth, D.S. Qin, A. Werner, J. Drechsel, B. Maennig, K. Leo, Appl. Phys. Lett. 81 (2002) 922.
[10] L.S. Hung, C.W. Tang, M.G. Mason, Appl. Phys. Lett. 70 (1997) 152.
[11] X. Zhou, M. Pfeiffer, J.S. Huang, J. Blochwitz-Nimoth, D.S. Qin, A. Werner, J. Drechesel, B. Maennig, K. Leo, Appl. Phys. Lett. 81 (2002) 922.
[12] R.H. Jordan, L.J. Rothberg, A. Dodabalapur, R.E. Slusher, Appl. Phys. Lett. 69 (1996) 1997.
[13] R. Meerheim, R. Nitsche, K. Leo, Appl. Phys. Lett. 93 (2008) 043310.
[14] L.S. Hung, L.R. Zheng, M.G. Mason, Appl. Phys. Lett. 78 (2001) 673.
[15] T. Hasegawa, S. Miura, T. Moriyama, T. Kimura, I. Takaya, Y. Osato, H. Mizutani, SID Symposium Digest of Technical Papers, vol. 35, 2004, p. 154.
[16] A.W. Dweydari, C.H.B. Mee, Phys. Status Solidi ppl. Res. 27 (1975) 223.
[17] C.L. Lin, H.W. Lin, C.C. Wu, Appl. Phys. Lett. 87 (2005) 021101.
[18] R. Meerheim, K. Walzer, M. Pfeiffer, K. Leo, Appl. Phys. Lett. 89 (2006) 061111.
[19] H. Aziz, Z.D. Popovic, N.X. Hu, A.M. Hor, G. Xu, Science 283 (1999) 1900.
[20] Z.D. Popovic, H. Aziz, A. Ioannidis, N. Hu, P.N.M. dos Anjos, Synth. Met. 123 (2001)179 123 (2001).
[21] Z.D. Popovic, H. Aziz, N. Hu, A. Ioannidis, P.N.M. dos Anjos, J. Appl. Phys. 89 (2001) 4673.